Archaeal orthologs of Cdc45 and GINS form a stable complex that stimulates the helicase activity of MCM

Yuli Xu[a,b,1], Tamzin Gristwood[c,1,2], Ben Hodgson[c,3], Jonathan C. Trinidad[d], Sonja-Verena Albers[e,4], and Stephen D. Bell[a,b,5]

[a]Molecular and Cellular Biochemistry Department, Indiana University, Bloomington, IN 47405; [b]Biology Department, Indiana University, Bloomington, IN 47405; [c]Sir William Dunn School of Pathology, Oxford OX13RE, United Kingdom; [d]Chemistry Department, Indiana University, Bloomington, IN 47405; and [e]Max Planck Institute für terrestrische Mikrobiologie, D-35043 Marburg, Germany

Edited by James M. Berger, Johns Hopkins University School of Medicine, Baltimore, MD, and approved October 12, 2016 (received for review August 18, 2016)

The regulated recruitment of Cdc45 and GINS is key to activating the eukaryotic MCM(2-7) replicative helicase. We demonstrate that the homohexameric archaeal MCM helicase associates with orthologs of GINS and Cdc45 in vivo and in vitro. Association of these factors with MCM robustly stimulates the MCM helicase activity. In contrast to the situation in eukaryotes, archaeal Cdc45 and GINS form an extremely stable complex before binding MCM. Further, the archaeal GINS•Cdc45 complex contains two copies of Cdc45. Our analyses give insight into the function and evolution of the conserved core of the archaeal/eukaryotic replisome.

DNA replication | CMG | Archaea | MCM | helicase

The initiation of DNA replication is an important control point in the progression of the cell cycle. In eukaryotes, origins are defined by the initiator protein ORC complex that, via the actions of two additional factors, the helicase coloaders Cdc6 and Cdt1, directs loading of the MCM(2-7) replicative helicase onto double-stranded DNA. Activation of the MCM(2-7) replicative helicase occurs subsequent to recruitment, leading to DNA melting and assembly of the full replisome apparatus (1, 2). Key steps in MCM activation involve a series of phosphorylation-dependent events that promote the sequential association of Cdc45 and the GINS complex with the chromatin-associated MCM double hexamer. These recruitment events are regulated by the CDK and DDK kinases and require the additional accessory factors Sld3/7, Dpb11, and Sld2(3-6). The Cdc45•MCM(2-7)•GINS complex (CMG) forms the core of the eukaryotic replisome, and this 11-subunit assembly appears to be the functional helicase driving fork progression (3–6). The archaeal replication machinery resembles an ancestral form of its eukaryotic counterpart. Archaea possess a simple homohexameric MCM (5, 7). In addition, archaeal homologs of GINS and Cdc45 have been identified (8–14). In species of the genus *Sulfolobus*, we have previously demonstrated that the GINS complex interacts with the N-terminal domains of MCM (8). In *Sulfolobus*, GINS is a dimer of dimers: one subunit, Gins23, is related to the eukaryotic GINS components Psf2 and Psf3, and the second *Sulfolobus* subunit, Gins15, is related to the eukaryotic Sld5 and Psf1. These sequence relationships have been confirmed by structural studies of the *Thermococcus kodakarensis* GINS complex that have demonstrated the tetrameric assembly of archaeal $(Gins15)_2$•$(Gins23)_2$ and validated the organizational similarity of the archaeal and eukaryotic GINS complexes (15). Interestingly, *Sulfolobus* GINS copurifies over the course of eight steps with a further polypeptide that we initially named RecJdbh, based on its observed homology with the presumptive DNA binding domain of the bacterial exonuclease, RecJ (8). Subsequent sequence analyses have revealed a relationship between RecJ and eukaryotic Cdc45, and this has been elegantly confirmed by recent structural studies of eukaryotic Cdc45 (9, 11, 16, 17). We therefore propose renaming RecJdbh as Cdc45. As archaea lack orthologs of Sld2, Sld3, Sld7, and Dpb11, and do not possess counterparts of CDK or DDK, it appears that Cdc45 may form a constitutive complex with GINS in cells. In the current work, we investigate the role of the Cdc45•GINS (hereafter CG) complex in vivo and in vitro. We observe association of CG with the MCM complex at replication origins and during replication fork progression. We map the interactions between Cdc45 and GINS and between the CG complex and MCM. We reveal that although neither Cdc45 nor GINS individually stimulates MCM activity, the formation of the full CMG complex robustly enhances the basal helicase activity of MCM. Our data indicate that the CMG helicase is a conserved and central component of the replication fork in archaea and eukaryotes.

Results

Generation of a Strain Expressing an Epitope Tagged Cdc45. To investigate the in vivo role of Cdc45 in DNA replication, we modified the endogenous *cdc45* gene of *Sulfolobus acidocaldarius* to encode a protein with a C-terminal dual affinity-tag (Fig. 1*A*). The addition of the C-terminal c-myc hexahistidine tag was confirmed by PCR amplification across the Saci_0177 gene (Fig. 1*B*), DNA sequencing, and Western blot analysis (Fig. 1*C*). The SacCdc45 strain displayed a similar growth rate compared with the parental strain (Fig. S1). Furthermore, analysis of the cell cycle profile by flow cytometry did not reveal any differences between the parental strain and SacCdc45 (Fig. S1). Thus, the C-terminal affinity tag to Cdc45 does not significantly perturb cell cycle progression.

Significance

For DNA to be duplicated, it must first be unwound. Here, we examine the nature of the helicase engine that drives this unwinding process. In archaea and eukaryotes, the core helicase is the MCM complex. Our studies reveal that the active form of the archaeal replicative helicase is a complex of MCM with the accessory proteins Cdc45 and GINS. Our work reveals functional conservation of this architecture despite the 2 billion-year evolutionary gulf between archaea and eukaryotes.

Author contributions: T.G., B.H., S.-V.A., and S.D.B. designed research; Y.X., T.G., B.H., and J.C.T. performed research; S.-V.A. contributed new reagents/analytic tools; Y.X., T.G., B.H., and S.D.B. analyzed data; and Y.X., T.G., B.H., and S.D.B. wrote the paper.

The authors declare no conflict of interest.

This article is a PNAS Direct Submission.

Freely available online through the PNAS open access option.

[1]Y.X. and T.G. contributed equally to this work.

[2]Present address: Oxford PharmaGenesis Ltd., Tubney, Oxford OX13 5QJ, United Kingdom.

[3]Present address: Cancer Research UK Manchester Institute, The University of Manchester, Manchester M20 4BX, United Kingdom.

[4]Present address: Molecular Biology of Archaea, Institute of Biology II, University of Freiburg, 79104 Freiburg, Germany.

[5]To whom correspondence should be addressed. Email: stedbell@indiana.edu.

This article contains supporting information online at www.pnas.org/lookup/suppl/doi:10.1073/pnas.1613825113/-/DCSupplemental.

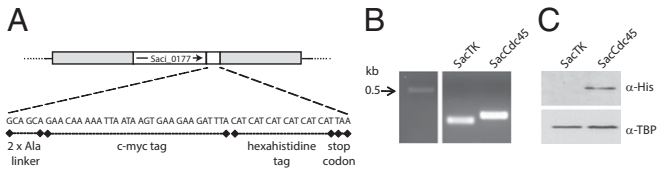

Fig. 1. Construction of strain SacCdc45, encoding chromosomally expressed affinity-tagged Cdc45. (*A*) Schematic of the DNA sequence insertion in SacCdc45. A DNA sequence encoding a c-myc and hexahistine affinity tag was integrated into the 3′ end of gene Saci_0177, encoding Cdc45, using a "pop-in, pop-out" approach. (*B*) PCR amplification across the 3′ end of Saci_0177 using a genomic DNA template generated 188- and 245-bp products in SacTK and SacCdc45, respectively, indicating successful insertion of the affinity-tag encoding sequence. (*C*) SacCdc45 expresses C-terminal affinity-tagged Cdc45. Western blot analysis was performed using whole-cell extracts from exponential cultures of the parental strain, SacTK, and SacCdc45, using an anti-His-tag antibody, and anti-TBP antibody as a control.

Cdc45 Interacts with GINS. Cdc45 was initially identified in *Sulfolobus solfataricus* during purification of the archaeal GINS complex, as Cdc45 was stably associated with the GINS proteins (8). After partial purification of Cdc45•His_6 from *S. acidocaldarius* using nickel affinity, gel filtration, and anion exchange chromatography, we detected two copurifying proteins (Fig. 2*A*). The coelution of Gins23 was confirmed by immunoblotting (Fig. 2*B*), and the proteins were identified by mass spectrometry as Gins15 (Saci_1278) and Gins23 (Saci_0901), both confirming the presence of a GINS•Cdc45 complex in *S. acidocaldarius* and demonstrating that the addition of the C-terminal tag had not disrupted formation of this complex.

We next performed yeast-two-hybrid analysis to examine the GINS–Cdc45 interaction in more detail (Fig. 2*C*). The Gins subunits contain an α-helical A domain and a β-strand rich B domain (14). The order of these domains is circularly permuted in Gins23 (BA) and Gins15 (AB) (Fig. S2). We could not observe any interaction between Gins23 and Cdc45, in agreement with our previous results (8). However, we confirmed interaction between Gin15 and Cdc45 and revealed that the C-terminal B domain of Gins15 was both necessary and sufficient for the interaction (Fig. 2*C*).

Cdc45 Is a Component of the *S. acidocaldarius* Replisome. Next we sought to determine whether Cdc45 is a component of the *S. acidocaldarius* replisome. To this end, we performed chromatin immunoprecipitation (ChIP) followed by quantitative PCR (qPCR) to determine the location of chromosomally associated Cdc45 and MCM throughout synchronous growth. qPCR was performed using 14 primer pairs for amplicons distributed across the SacCdc45 genome, including primers targeting the three origins of replication. MCM has previously been shown to be recruited to the *S. acidocaldarius* origins of replication at initiation of DNA replication (18), and as the presumed replicative helicase, MCM would be predicted to travel with the moving replication forks during S phase.

SacCdc45 strains were synchronized using the baby machine method (18). After formaldehyde-fixation, ChIP was performed using anti-MCM and anti-myc antibodies from cells fixed in G1/early S-phase, mid-S-phase and G2 phase (Fig. 3*A*). These experiments indicated recruitment of MCM and Cdc45 to the three origins of replication (*oriC1*, *oriC2*, and *oriC3*) in G1/S phase (Fig. 3 *B* and *C*). ChIP signals from the mid-S-phase samples reveal a relative reduction in Cdc45 and MCM at all three origins and relative increases in the interorigin regions. This is consistent with a model in which MCM and Cdc45 are associated with moving replication forks.

This model is also supported by the observed occupancy of Cdc45 and MCM at the region midway between the two most separated origins (*oriC2* and *oriC3*; ∼1,727 kb apart). This is the last region of *S. acidocaldarius* chromosome to be replicated (18). The ChIP signal from S phase cells indicates that replication forks have not yet progressed to this region in a significant number of cells (Fig. 3*D*). However, by the latest time (210 min), the moving forks, containing Cdc45 and MCM, have now reached this final region of DNA in a large number of cells (Fig. 3*E*). We note that flow cytometry reveals that some of the population has reentered G1 by 210 min; concomitant with this, we observe new enrichment of MCM and Cdc45 at the origins.

The CG Complex Is a Heterohexameric Assembly. Next, we sought to determine the biochemical effect of CG association with MCM. Despite numerous attempts to express Cdc45 in a variety of bacterial and eukaryotic systems, we were unable to prepare the protein as recombinant from a heterologous system. Although it was possible to exploit the SacCdc45 strain to express a His-tagged version of Cdc45 from the endogenous locus, we could only obtain yields of a

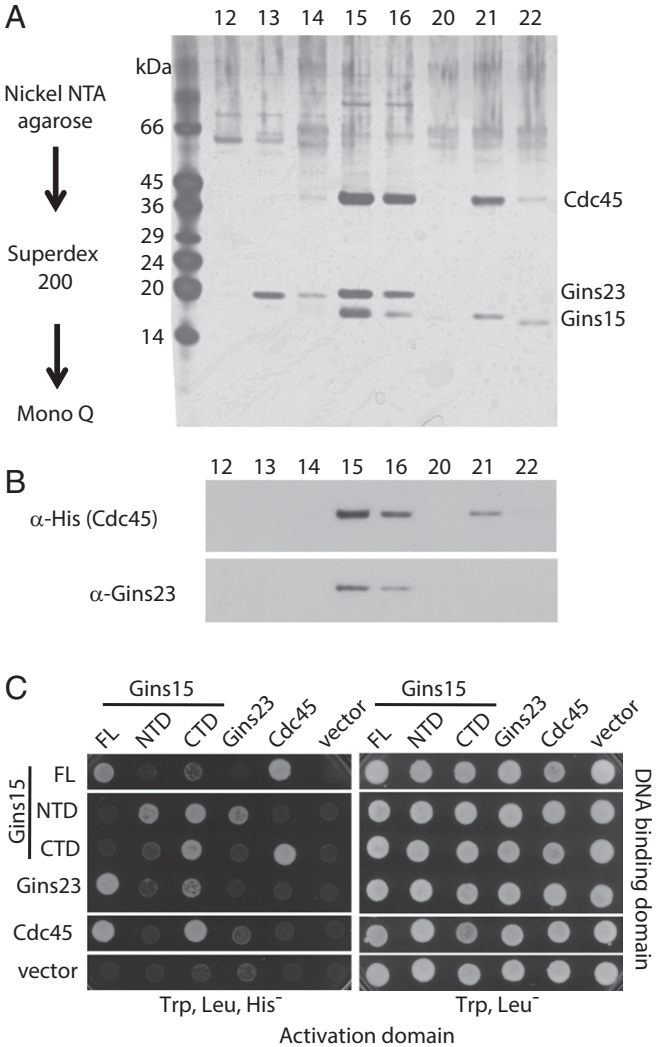

Fig. 2. Cdc45 forms a complex with Gins15 and Gins23 in vivo. (*A*) Partial purification of the CG complex from extracts by successive affinity, size exclusion, and anion exchange chromatography; a silver-stained gel of the peak fractions from the final column is shown. (*B*) Western blotting was performed on the peak fractions from *A*, using the indicated antisera. (*C*) Yeast 2 hybrid analyses of interactions between the N- and C-terminal domains of Gins15 and full-length Gins23 and Cdc45. Growth on the selective plates (lacking histidine) is indicative of interaction.

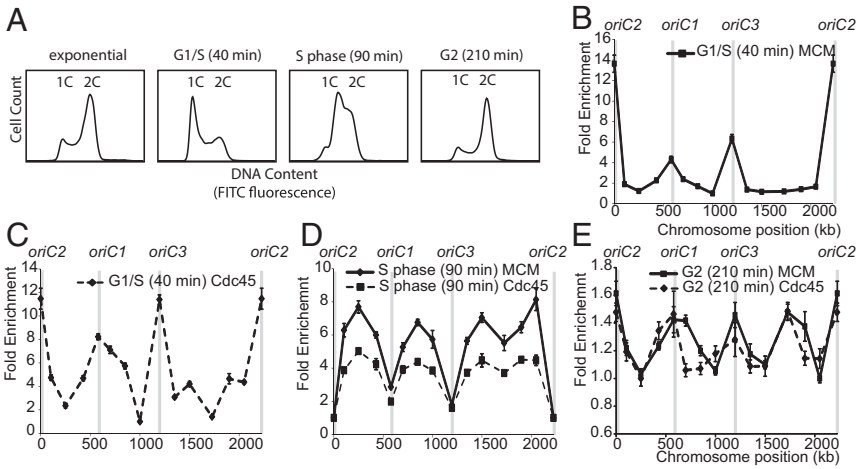

Fig. 3. ChIP reactions using synchronized SacCdc45 cells were used to examine genomic localization of Cdc45 and MCM during the cell cycle. (*A*) Flow cytometry profiles of asynchronous, G1/early S-phase, S-phase, and G2-enriched synchronized cell populations are indicated. (*B–E*) ChIP profiles showing the enrichment of DNA in the immunoprecipitates at the various genomic loci at the indicated times.

few hundred nanograms of protein from 6 L of culture. Accordingly, we switched to using the related strain *Sulfolobus islandicus* for our biochemical studies. Exploiting a strong and controllable promoter, we were able to express and purify milligram-scale amounts of C-terminally His-tagged Cdc45. We combined this with bacterially expressed GINS complex and recovered a reconstituted CG. Size exclusion chromatography of the reconstituted material reveals the majority of the CG complex has a mobility compatible with a 2:2:2 stoichiometry of Gins15:Gins23:Cdc45 (Fig. 4*A*). To further confirm the composition of the CG complex, we performed native electrospray ionization mass spectrometry (Fig. 4*B*). A 2:2:2 (Gins15:Gins23:Cdc45) complex has a predicted mass of 158,002 Da, whereas a 2:2:1 complex would have a mass of 117,346 Da, and the observed mass is 161,800, supporting the 2:2:2 stoichiometry. The excess mass that we detect is likely a result of tightly associated solvent molecules and ions.

To test the stability of the CG complex, we immobilized it on Ni-NTA agarose beads. We then subjected it to washing in a variety of buffers, ranging in ionic concentration up to 1 M NaCl and with up to 8 M urea. Remarkably, the complex remained intact even when subjected to four washes containing 8M urea (Fig. 4*C*).

The CG Complex Interacts with MCM. Next, we performed pulldown experiments, exploiting the His-tag on Cdc45, and could detect interaction between full-length MCM and the CG complex (Fig. 4*D*). No stable interaction was detectable with Cdc45 alone in the absence of GINS. Our previous work has demonstrated that Gins23 interacts with the N-terminal domains of MCM (8). The MCM N-terminal region can be further subdivided to A and B/C domains (19). Further, structural studies of eukaryal CMG have implicated the A domains of MCM2 and MCM5 as being of importance for CMG formation (3). We observe that deletion of the A domain of *S. islandicus* MCM abrogates association with CG (Fig. 4*D*). Interestingly, although the A domain is necessary for interaction, it is not sufficient. Using GST fusions of the N-terminal domains of MCM (domains A and B/C), and truncated derivatives thereof, we observe interaction mediated by the intact N-terminal domain, but this is abolished by deletion of either A or B/C domains (Fig. 4*E*). We also tested whether ATP•Mg or inclusion of single-stranded or Y-shaped oligonucleotides could influence the association of CG with MCM (Fig. 4*F*). Quantitation of the band intensity using ImageJ revealed a 2.5-fold enhancement of MCM retention on the CG beads by inclusion of fork-shaped DNA, single-stranded DNA, or nucleotide cofactor. The presence of either DNA with ATP resulted in a six- to sevenfold enrichment of MCM.

The Addition of CG Stimulates the Helicase Activity of MCM. We sought to determine whether the CG complex has any effect on the ATPase or DNA binding activities of MCM. We examined DNA binding to a Y-shaped oligonucleotide substrate (Fig. 5*A*). Addition of CG resulted in a very slight (less than 1.5-fold) enhancement of the DNA binding activity of the MCM complex. We could not detect any DNA binding by the isolated CG complex. Next, we examined the influence of CG on the ATPase rate of MCM. The *S. islandicus* MCM has an intrinsic ATPase activity that is not affected by the addition of single-stranded DNA (Fig. 5*B*). Addition of CG lowers the basal ATPase rate by a factor of three, and addition of DNA now results in a ∼1.5-fold stimulation of ATPase activity.

Next, we determined whether CG, GINS, or Cdc45 could influence the helicase activity of MCM. At the concentrations of MCM we used in these experiments, we detect very low levels of activity by MCM alone (∼7% of template unwound). The addition of increasing concentrations of CG resulted in a clear stimulation of MCM helicase activity (Fig. 5*C*). Importantly, the CG complex alone had no helicase activity, and addition of a nonspecific control, BSA, failed to stimulate helicase activity. Next we tested whether GINS or Cdc45 could individually affect MCM's helicase activity (Fig. 5*D*). Addition of GINS complex or Cdc45 individually had no detectable effect on the yield of product. Intriguingly, previous studies have yielded contrasting results on whether archaeal GINS can or cannot stimulate the helicase activity of MCM (8, 20–22). However, we observed a strong stimulation of helicase activity as we added the Cdc45•GINS complex to the reaction. Importantly, deletion of the A domain of MCM abolishes the stimulatory effect of CG on MCM's helicase activity (Fig. 5*E*). We note that deletion of the A domain has no significant effect on the inherent helicase activity of MCM (23). Thus, association of the CG complex with MCM results in robust helicase activity.

Discussion

We provide a characterization of an archaeal CMG complex in vivo and in vitro. We demonstrate that Cdc45 and GINS form a stable complex in a range of species. Further, this complex associates with MCM at replication origins at the onset of replication and colocalizes with MCM during replication elongation. In agreement with our previous data, but in contrast with other reports, neither GINS nor Cdc45 individually affect MCM's helicase

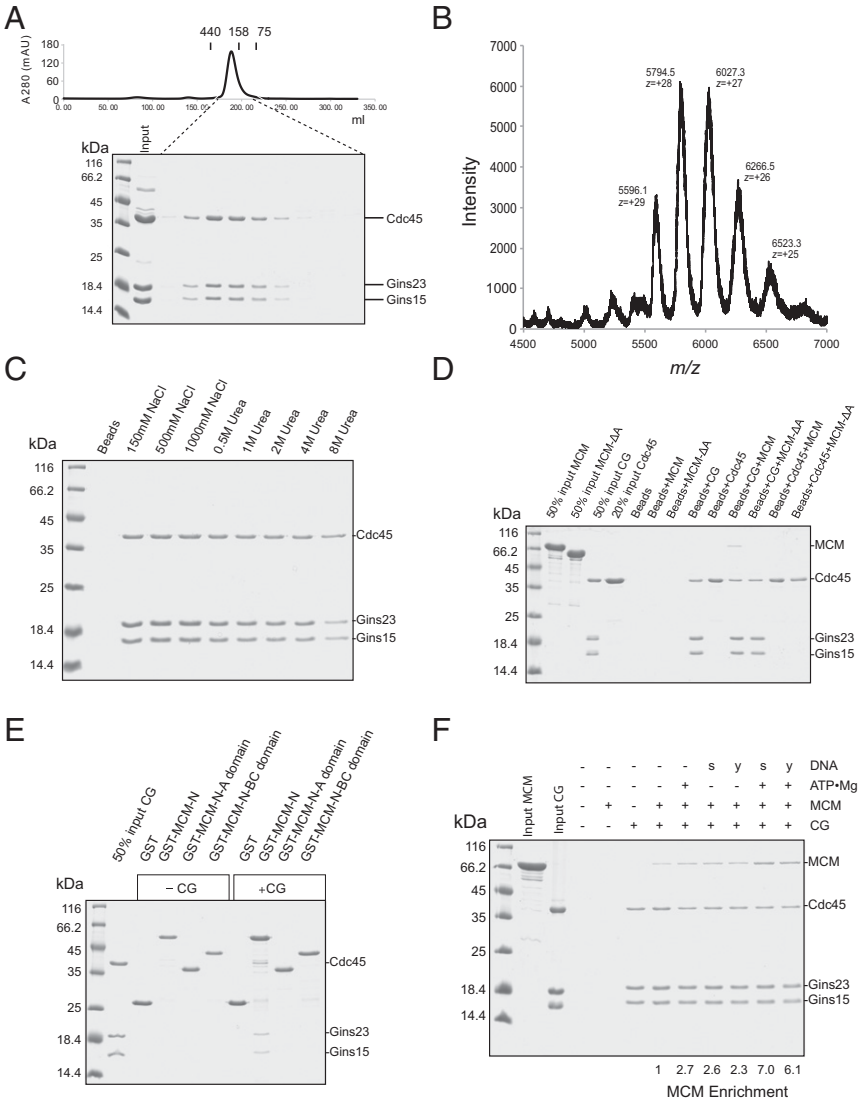

Fig. 4. (*A*) Gel filtration analysis of the reconstituted recombinant CG complex. The CG complex was analyzed by gel filtration on a Superdex 200 26/60 column. The UV absorption profile is shown with the positions of elution of 440, 158, and 75 kDa size standards (ferritin, aldolase, and conalbumin, respectively) indicated. (*Bottom*) SDS PAGE analysis of the corresponding fractions. (*B*) Native electrospray ionization mass spectrometry profile for the CG complex. The peak at m/z = ~5,794.5 has a charge of +28. (*C*) Stability of the CG complex: 11 μg CG complex immobilized on Ni-NTA beads were washed four times with 500 μL TBS (10 mM Tris at pH 8.0, 150 mM) or TBS supplemented with NaCl or urea to the indicated concentration. The bead-retained material was analyzed by SDS/PAGE and proteins stained with Coomassie Brilliant Blue. (*D*) Pulldown assays to test for interaction between 13 μg Cdc45 or the CG complex immobilized on Ni-NTA via the His-tag on Cdc45 and 18 μg MCM or MCM-ΔA. (*E*) Interactions between the N-terminal domains of MCM and the CG complex. Glutathione sepharose beads bound to GST, GST-fused to MCM-N (residues 1–265), MCM-*N*-A domain (residues 1–104), or MCM-*N*-BC (residues 105–265) were incubated with 13 μg CG complex. After incubation and washing, bead-retained material was examined by SDS PAGE. (*F*) Ni-NTA pulldown assays with the indicated combination of CG complex, MCM, and ATP•Mg (2 mM final) and 20 μM single-stranded (s) or 10 μM Y-shaped DNA (y) (the distinct concentrations were to ensure same bulk amount of DNA per reaction). The relative enrichment of MCM was calculated by measuring band intensity of MCM, using ImageJ, and normalizing to the Cdc45 band intensity.

activity (8). However, the CG complex promotes a robust stimulation of MCM's helicase activity, and we can readily detect interaction between CG and MCM, using physical assays.

The proposed evolutionary relationship between RecJ and Cdc45 has been recently confirmed by structural studies. Cdc45 possesses the RecJ signature DHH and DHHA1 motifs, separated by a eukaryotic Cdc45-specific region termed the CMG interaction domain (CID) (24). We performed HHPred analysis and detected a highly significant homology ($P = 3.1 \times 10^{-11}$) between residues 20–335 of *S. solfataricus* Cdc45 and bacterial RecJ (Fig. S3*A*). However, to our considerable surprise, we also observed a significant relationship (*P* value = 0.00051 for relationship to *Arabidopsis* Cdc45) predicted by HHpred between residues 80–339 of *S. solfataricus* Cdc45 and the CID of eukaryal Cdc45s (Fig. S3 *B* and *C*).

Thus, *Sulfolobus* Cdc45 is related both to the RecJ fold of eukaryotic Cdc45 and the CID (Fig. 6 and *SI Materials and Methods*). We speculate, therefore, that during the evolution of eukaryal Cdc45, a gene duplication and matryoshka-like internal fusion event occurred, with the CID subsequently diverging from the ancestral archaeal Cdc45 sequence. Thus, we suggest that the single eukaryal Cdc45 actually corresponds to two divergent copies of the archaeal ancestor. In agreement, we observe that the archaeal CG complex contains two copies of Cdc45, in contrast to the single Cdc45 in the eukaryotic assembly. The archaeal GINS complex is a dimer of dimers, and therefore is inherently more

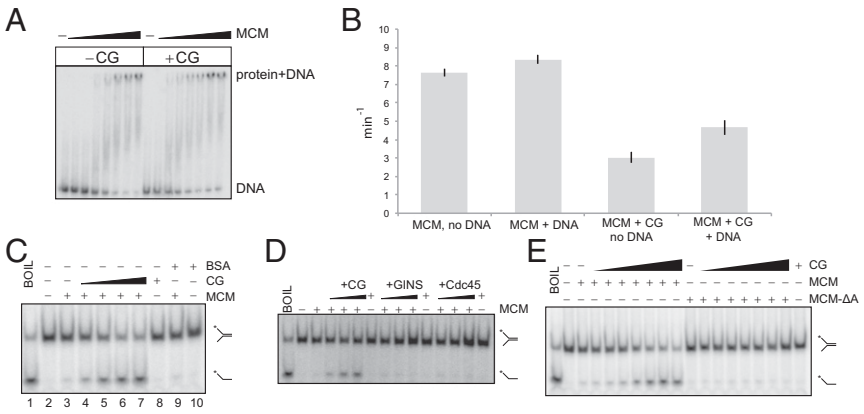

Fig. 5. Effect of CG on the biochemical properties of MCM. (*A*) EMSA analysis of MCM binding to 2 nM Y-shaped oligonucleotide DNA in the presence and absence of 500 nM CG. MCM concentrations were 5, 7.5, 10, 12.5, 15, 17.5, and 20 nM hexamer. (*B*) ATPase measurements of 100 nM MCM (hexamer) supplemented with 1 μM CG or corresponding buffer control. Where added, single-stranded DNA was at 1 μM. (*C*) DNA helicase assays with MCM and CG complex. DNA substrate was 1 nM. MCM was at 20 nM as hexamer; increasing amounts (125, 250, 500, 1,000 nM) of CG complex and 1 μM BSA as indicated were added. The control lane with CG complex alone had CG at 1 μM. (*D*) DNA helicase assays for MCM with CG complex, GINS, and Cdc45 separately. MCM was added 20 nM as hexamer; increasing amounts (125, 250, 500 nM) of CG complex, GINS, and Cdc45, as indicated, were added. Reactions with CG, GINS, or Cdc45 contained the indicated protein at 500 nM. (*E*) DNA helicase assays with MCM, MCM-ΔA, and CG complex. MCM and MCM-ΔA were added to 20 nM as hexamer; increasing amounts (15, 31, 62, 125, 250, 500, 1,000 nM) of CG complex, as indicated, were added. CG alone in a reaction without MCM or MCM-ΔA was at 1 μM.

symmetric than the eukaryotic heterotetrameric GINS (8, 15). Archaeal GINS thus possesses two copies of the Gins15 C-terminal B domain we have demonstrated interacts with Cdc45. In eukaryotes, during the diversification of Psf1 and Sld5, presumably the progenitor ancestral Cdc45 interaction site on Sld5 has diverged and lost the ability to interact with Cdc45 (3). It is conceivable that this domain of Sld5 now plays a distinct and eukaryotic-specific role in orchestrating the replisome architecture. Indeed, we note that a yeast 2-hybrid study has provided evidence that *Drosophila melanogaster* Sld5 interacts with MCM10, a factor that lacks homologs in archaea. However, the region of Sld5 responsible for this interaction has not been mapped (25).

The greater symmetry in the archaeal CG complex is mirrored in the homohexameric MCM in archaea. In eukaryotes, CG appears to latch a gate between MCM2 and MCM5 (3). We have recently demonstrated that an open ring form of archaeal MCM is preferentially recruited to replication origins (26). We propose, therefore, that the archaeal CG complex will act similarly to its eukaryotic ortholog, conceivably facilitating closure of the gate in the archaeal MCM after its loading on replication origins.

Modeling of the human Cdc45 crystal structure into EM maps of CMG indicates that human Cdc45 makes multiple protein–protein contacts within the CMG assembly (24). More specifically, the DHH domain contacts the B domain of Psf1, whereas the CID mediates contacts with both Psf2 and MCM subunits. Our observations indicate that *S. acidocaldarius* Cdc45 is restricted to interactions with the Gins15 subunit. Thus, the eukaryotic Psf1–DHH interaction appears to be the key conserved feature of this assembly. Although we acknowledge that our binary interaction studies may have overlooked interactions important in the context of a higher-order CMG assembly, it is possible that during the evolution of the eukaryal CID, this region of Cdc45 acquired the ability to interact with Psf2 and its specific eukaryotic MCM subunit partners.

Our observations that Cdc45 and GINS form a remarkably stable complex both as recombinant proteins and in cell-free extracts highlight another key difference from the situation in eukaryotes. The sequential recruitment of eukaryal Cdc45 and GINS provide key control points for the cell cycle–dependent regulation of the activation of DNA replication (1, 2). This greater regulatory potential in the eukaryal assembly pathway presumably reflects the increased requirement for fidelity of control for the multiplicity of replication origins in eukaryotic chromosomes. It remains to be determined whether the recruitment of CG is a control point in the *Sulfolobus* cell cycle. *Sulfolobus* species have three replication origins per chromosome, and our work in *S. islandicus* has revealed that each is specified by a distinct initiator protein (23, 24). We have demonstrated control at the level of the initiator protein for one of these origins, *oriC1*, and this mechanism likely extends to *oriC2*. How initiation at *oriC3*, an orc1/cdc6-independent origin, is regulated is currently unknown. Given that the first common feature of all three origins is the recruitment of MCM, we speculate that MCM activation could be a key point for coordinate control of firing of all three origins. We note that we detect maximal stimulation of MCM's helicase activity at a ratio of 25 molecules of GINS•Cdc45 per hexamer of MCM. Although this may simply reflect binding affinity in our in vitro assays conditions, it is conceivable that regulatory modifications to MCM and/or CG components in vivo could affect the strength of interaction we

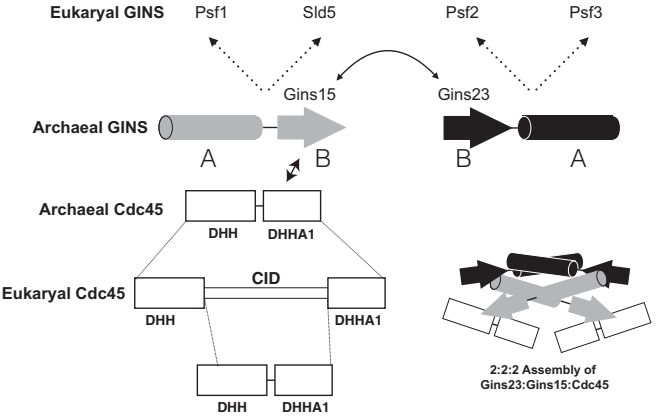

Fig. 6. Evolutionary relationships and interactions between archaeal/eukaryotic GINS and Cdc45. Physical interactions between components are shown as double-headed solid arrows. Evolutionary relationships are shown as dotted lines. The diagram in the lower right provides a model for the 2:2:2 assembly of Gins23:Gins15:Cdc45, with the two copies of Cdc45 interacting with distinct Gins15 subunits via the latter's B domain.

observe. Such a mode of regulation could provide a mechanism for the coordinate control of the three disparate origins present in the *Sulfolobus* chromosome (27).

Methods

Cell Growth. *S. acidocaldarius* SacTK, a *pyrEF*$^{-}$ TK^{+} strain derived from *S. acidocaldarius* DSM639 (28), was grown at 75 °C in Brock's medium at pH 3.2 containing 0.1% (wt/vol) tryptone, 0.2% (wt/vol) xylose, and 0.025 mg/mL uracil. After transformations, SacTK cultures contained 0.1% NZ-amine as an alternative to tryptone. When required, Brock's medium was solidified with 0.7% Gelrite (GmbH). Transformations with of *S. islandicus* with expression plasmid pSSR-Cdc45 and subsequent growth were as described (29). Yeast two-hybrid assays were performed in strain AH109, as described in the Matchmaker handbook (Clontech).

Genetic Manipulation of *Sulfolobus*. The construct for tagging *S. acidocaldarius cdc45* was generated by overlap PCR (Table S1) and transformation of *S. acidocaldarius* strain SacTK (28). Cdc45 was overexpressed in *S. islandicus* E223S, using the pSSR vector (23). For detailed information, see *SI Materials and Methods*.

Protein Purification. For details of the purification methods, see *SI Materials and Methods*. Briefly, *S. acidocaldarius* CG complex was purified by metal affinity, size exclusion, and chromatography anion exchange. GST-fusion proteins (GST-MCM-N, GST-MCM-*N*-A domain, GST-MCM-*N*-BC domain) were purified using glutathione sepharose (for details, see *SI Materials and Methods*). Recombinant MCM and MCM ΔA were purified by chromatography over heparin sepharose and gel filtration matrices.

Intact Protein Complex Mass Spectrometry. The CG complex was prepared in 50 mM ammonium acetate at a concentration of 4.4 μM. The sample was infused into a Synapt G2S mass spectrometer equipped with a nano ESI source at 0.5 μL/min. The source conditions were as follows: capillary voltage, 1.5 kV; source temperature, 100 °C; sampling cone, 80 V; source offset, 80 V; desolvation temperature, 150 °C; nanoflow gas pressure, 0.5 Bar. To promote declustering of solvent ions from the complex, the trap and transfer collision energies were varied between 70 and 100 V. The data were processed in MassLynx (Waters Corporation). Results from 5 min of scanning was averaged and smoothed, using the Savitzky Golay algorithm with four channels and 20 rounds of smoothing (30). To determine the mass of the intact complex, the data were processed using MaxEnt 1 (Waters Corporation), with a resolution of 10 Da/channel and damage model with a uniform Gaussian half height of 40 Da.

Pulldown Assays. Pulldown assays used either beads with Ni-NTA–coupled protein or glutathione sepharose–coupled proteins.

ATPase, EMSA, and Helicase Assays. These procedures are detailed in *SI Materials and Methods*. ATPase rate was assessed by colorimetry and EMSA, and helicase assays were essentially as described previously (20), with the exception of the inclusion of 75 mM NaCl in the binding and reaction buffers.

ChIP Experiments. The procedure for ChIP assays is described in detail in *SI Materials and Methods* (26). ChIP was performed using anti-MCM or anti-c-myc antibodies, as described previously (18). The resulting purified DNA was quantified by qPCR.

ACKNOWLEDGMENTS. We thank Luca Pellegrini for informative discussions about human Cdc45. We also thank Rachel Whitaker, University of Illinois, for sharing data before publication. We are indebted to Marleen van Wolferen with help with the *S. acidocaldarius* genetics. We thank the Biotechnology and Biological Sciences Research Council, Wellcome Trust, Max Planck Society, and Indiana University College of Arts and Sciences for funding.

1. Siddiqui K, On KF, Diffley JF (2013) Regulating DNA replication in eukarya. *Cold Spring Harb Perspect Biol* 5(9):a012930.
2. Tanaka S, Araki H (2013) Helicase activation and establishment of replication forks at chromosomal origins of replication. *Cold Spring Harb Perspect Biol* 5(12):a010371.
3. Costa A, et al. (2011) The structural basis for MCM2-7 helicase activation by GINS and Cdc45. *Nat Struct Mol Biol* 18(4):471–477.
4. Ilves I, Petojevic T, Pesavento JJ, Botchan MR (2010) Activation of the MCM2-7 helicase by association with Cdc45 and GINS proteins. *Mol Cell* 37(2):247–258.
5. Bell SD, Botchan MR (2013) The minichromosome maintenance replicative helicase. *Cold Spring Harb Perspect Biol* 5(11):a012807.
6. Moyer SE, Lewis PW, Botchan MR (2006) Isolation of the Cdc45/Mcm2-7/GINS (CMG) complex, a candidate for the eukaryotic DNA replication fork helicase. *Proc Natl Acad Sci USA* 103(27):10236–10241.
7. Kelman LM, Kelman Z (2014) Archaeal DNA replication. *Annu Rev Genet* 48:71–97.
8. Marinsek N, et al. (2006) GINS, a central nexus in the archaeal DNA replication fork. *EMBO Rep* 7(5):539–545.
9. Sanchez-Pulido L, Ponting CP (2011) Cdc45: The missing RecJ ortholog in eukaryotes? *Bioinformatics* 27(14):1885–1888.
10. Li Z, et al. (2011) A novel DNA nuclease is stimulated by association with the GINS complex. *Nucleic Acids Res* 39(14):6114–6123.
11. Makarova KS, Koonin EV, Kelman Z (2012) The CMG (CDC45/RecJ, MCM, GINS) complex is a conserved component of the DNA replication system in all archaea and eukaryotes. *Biol Direct* 7:7.
12. Labib K, Gambus A (2007) A key role for the GINS complex at DNA replication forks. *Trends Cell Biol* 17(6):271–278.
13. Onesti S, MacNeill SA (2013) Structure and evolutionary origins of the CMG complex. *Chromosoma* 122(1-2):47–53.
14. MacNeill SA (2010) Structure and function of the GINS complex, a key component of the eukaryotic replisome. *Biochem J* 425(3):489–500.
15. Oyama T, et al. (2011) Architectures of archaeal GINS complexes, essential DNA replication initiation factors. *BMC Biol* 9:28.
16. Yuan Z, et al. (2016) Structure of the eukaryotic replicative CMG helicase suggests a pumpjack motion for translocation. *Nat Struct Mol Biol* 23(3):217–224.
17. Abid Ali F, et al. (2016) Cryo-EM structures of the eukaryotic replicative helicase bound to a translocation substrate. *Nat Commun* 7:10708.
18. Duggin IG, McCallum SA, Bell SD (2008) Chromosome replication dynamics in the archaeon Sulfolobus acidocaldarius. *Proc Natl Acad Sci USA* 105(43):16737–16742.
19. Fletcher RJ, et al. (2003) The structure and function of MCM from archaeal M. Thermoautotrophicum. *Nat Struct Biol* 10(3):160–167.
20. Lang S, Huang L (2015) The Sulfolobus solfataricus GINS complex stimulates DNA binding and processive DNA unwinding by minichromosome maintenance helicase. *J Bacteriol* 197(21):3409–3420.
21. Ogino H, et al. (2014) Activation of the MCM helicase from the thermophilic archaeon, Thermoplasma acidophilum by interactions with GINS and Cdc6-2. *Extremophiles* 18(5): 915–924.
22. Yoshimochi T, Fujikane R, Kawanami M, Matsunaga F, Ishino Y (2008) The GINS complex from Pyrococcus furiosus stimulates the MCM helicase activity. *J Biol Chem* 283(3):1601–1609.
23. Barry ER, McGeoch AT, Kelman Z, Bell SD (2007) Archaeal MCM has separable processivity, substrate choice and helicase domains. *Nucleic Acids Res* 35(3):988–998.
24. Simon AC, Sannino V, Costanzo V, Pellegrini L (2016) Structure of human Cdc45 and implications for CMG helicase function. *Nat Commun* 7:11638.
25. Gouge CA, Christensen TW (2010) Drosophila Sld5 is essential for normal cell cycle progression and maintenance of genomic integrity. *Biochem Biophys Res Commun* 400(1):145–150.
26. Samson RY, Abeyrathne PD, Bell SD (2016) Mechanism of Archaeal MCM helicase recruitment to DNA replication origins. *Mol Cell* 61(2):287–296.
27. Samson RY, et al. (2013) Specificity and function of archaeal DNA replication initiator proteins. *Cell Reports* 3(2):485–496.
28. Gristwood T, Duggin IG, Wagner M, Albers SV, Bell SD (2012) The sub-cellular localization of Sulfolobus DNA replication. *Nucleic Acids Res* 40(12):5487–5496.
29. Zheng T, et al. (2012) Development of a simvastatin selection marker for a hyperthermophilic acidophile, Sulfolobus islandicus. *Appl Environ Microbiol* 78(2):568–574.
30. Savitzky A, Golay MJE (1964) Smoothing and differentiation of data by simplified least squares procedures. *Anal Chem* 36(8):1627–1639.
31. Brewster AS, et al. (2008) Crystal structure of a near-full-length archaeal MCM: Functional insights for an AAA+ hexameric helicase. *Proc Natl Acad Sci USA* 105(51): 20191–20196.